



Published in final edited form as:

Chem Commun (Camb). 2016 May 7; 52(37): 6332–6335. doi:10.1039/c6cc02282k.

Minimal C-Terminal Modification Boosts Peptide Self-Assembling Ability for Necroptosis of Cancer Cells

Zhaoqianqi Feng, Huaimin Wang, Xuwen Du, Junfeng Shi, Jie Li, and Bing Xu

Department of Chemistry, Brandeis University, 415 South Street, Waltham, Massachusetts 02454, United States

Abstract

Here we reported the first case that enhancing self-assembling ability boosts anti-cancer efficacy through simple and minimal modification of C-terminal of a D-tripeptide. By only 2% change of the molecular weight, this facile approach increases the inhibitory activity over an order of magnitude (IC_{50} from 431 to 23 μ M) towards an osteosarcoma cell line.

The ideal cancer therapeutics should selectively kill cancer cells without harming normal cells. Current chemotherapy for cancer treatment, however, still falls short of that goal. For example, cisplatin (CDDP), a well-established clinical anticancer drug, causes myelosuppression.¹ Another extensively used anticancer drug, paclitaxel, exhibits toxic effect on the bone marrow.² The recent success in immunotherapy relies on the actions of antibodies,³ has yet to be extended to the tumors that express low level cancer specific antigens.⁴ These limitations call for paradigm-shifting approaches for the development innovative chemotherapeutics of cancer treatment. To meet this need, we and others are developing anticancer nanomedicine based on the enzyme-instructed supramolecular assemblies of small molecules,^{5, 6–9} which represents a new approach that departs from the current dogma of tight and specific ligand-receptor interactions. For example, the assemblies of small molecules even can inhibit cancer cells selectively.^{10, 11} These encouraging results have led to the development of enzyme-instructed self-assembly (EISA),¹² which selectively generates assemblies of small molecules (e.g., small peptide derivatives^{6, 9} or carbohydrate derivatives⁸) *in-situ* on cancer cells for killing the cancer cells. Despite these advancements, the concentrations of those molecules required for inhibiting cancer cells still are quite high (e.g., 300–500 μ M).^{6–8} Thus, there is a need of an effective strategy to increase the efficacy of self-assembling molecules for cancer inhibition.

Because it is the *in-situ* formation of supramolecular assemblies to kill cancer cells,^{11, 12} a logical approach for increasing the inhibitory efficacy is to enhance the self-assembling ability of the building blocks. Although elongating the peptides improves the self-assembling ability of peptides,¹² it adds up the molecular weight, which thwarts the purpose of reducing the therapeutic dosage. Thus, we choose to use a neutral small functional group replacing the carboxylic acid group at the C-terminal of the peptides for enhancing the self-

assembling ability of the peptides (Fig. 1). Despite the simplicity of this approach, it receives little attention for designing self-assembling molecules.¹³ The results of this work reveal that such a simple and minimal modification of C-terminal of a D-tripeptide significantly enhance the self-assembling ability of the peptide, which increases their efficacy of cancer cell inhibition over an order of magnitude, even results in a IC_{50} to be comparable to that of cisplatin and more potent than carboplatin towards an osteosarcoma cell line.^{14, 15} Using different C-terminal groups, we further confirm the correlation between self-assembling ability and the inhibitory activity of the D-tripeptides. Moreover, this modification preserves the exceptional selectivity of enzyme-instructed self-assembly for inhibiting cancer cells. In addition, we confirm that the supramolecular assemblies on the cancer cells induce cell necroptosis, a recently defined modality of cell death.¹⁶ This work illustrates a facile strategy to explore self-assembling molecules for selectively killing cancer cells via enzymatic reactions.

To prove the concept that enhancing self-assembling ability boosts inhibitory efficacy, we choose a naphthyl-capped D-tripeptide derivative (**4**)⁶ as the parent compound. As shown in Fig. 1, we select N-methylacetamide (-CONHMe), acetohydrazide (-CONHNH₂), and methylacetate (-COOMe) groups to replace the carboxylic acid terminal of **4** to result in D-tripeptide derivatives **1**, **2**, and **3**, respectively. Based on that phosphatase-instructed self-assembly of **4** selectively kills cancer cells,^{6-8, 17} we choose to phosphorylate the D-Tyr in **1**, **2**, **3** and **4** to generate the corresponding precursors, **1p**, **2p**, **3p** and **4p**. Being different in structural and chemical properties, these C-terminal groups provide a set of representative molecules to validate the molecular design in Fig. 1. From **4p** to **1p**, **2p**, and **3p**, the molecular weights increase less than 2%. According to those structures, we combine solid phase peptide synthesis (SPPS) and solution phase synthesis to produce **1p**, **2p**, **3p**, and **4p** in fair yields (Scheme S1).

After obtaining the precursors, we examine the self-assembly ability of those four D-peptide derivatives in water via enzymatic dephosphorylation of their corresponding precursors. Using hydrogelation as a simple assay to test the molecular self-assembly in water,¹² we find that, at the concentration of 1 mM and pH 7.4, all the four precursors form transparent solutions. After the addition of alkaline phosphatase (ALP, 3U/mL), the solution of **1p** or **2p** turns into a hydrogel, the solution of **3p** forms a suspension, and the solution of **4p** becomes more viscous (Fig. S5). This result suggests that **1**, **2**, and **3** possess higher self-assembling ability than **4** does. Transmission electron microscopy (TEM) reveals that, after their enzymatic formation, **1**, **2**, **3** and **4** self-assembles to result in nanofibers with the diameter of 10.6 ± 2 , 9.7 ± 2 , 17.4 ± 2 and 6.2 ± 2 nm, respectively (Fig. 2). Compared with **1**, **2**, and **3**, **4** yields much thinner but uniform nanofibers, further indicating that **4** has relatively weaker self-assembly ability. In addition, **3** self-assembles to form bundles of short nanofibrils, which is consistent with the suspension after adding ALP in the solution of **3p**. These results confirm the higher self-assembling abilities of **1**, **2**, and **3** than that of **4**.

To further examine the enhancement of self-assembling ability, we use rheometer to compare the viscoelastic properties of hydrogels formed by **1**, **2**, **3** and **4** upon adding ALP in the solutions of their corresponding precursors (0.5 wt%). As shown in Fig. 3A, the addition of ALP into the solution of **4p** causes the storage modulus (G') to intersect with loss

modulus (G'') at around 0.4 hours, indicating the gelation point of **4**. However, immediately after mixing ALP with the solution of **1p**, **2p** or **3p**, G' is greater than G'' (i.e., $G' > G''$ at $t=0$), indicating that **1**, **2**, or **3** already reaches its gelation point immediately after mixing. These rheological results confirm that minimal C-terminal modification of **4** boosts the self-assembling ability of the resulting short peptides. To further compare the self-assembling abilities of **1**, **2**, **3**, and **4** below their gelation concentrations, we use static light scattering (SLS) to assess the self-assembly of those D-tripeptide derivatives before and after the enzymatic dephosphorylation. As shown in Fig. 3B, the addition of ALP into the solution of each precursor results in significant increase of SLS signals, indicating enzyme-instructed self-assembly. The increases of the SLS signals depends on the concentrations of the precursors. At 12.5 μM , SLS suggests the self-assembling abilities follow the order of $3 > 1 > 4$. At 25 μM , the SLS signals of **3p** and **3** change little, suggesting that **3** starts to precipitate, agreeing with the observation of suspension after adding ALP to the solution of **3p** (*vide supra*); SLS signals of **2** increases more than that of **4** does, but still less than that of **1**. This result indicates that the self-assembling abilities follow the order of $3 > 1 > 2 > 4$. At 50 μM , the SLS signal of **1p** starts increasing, indicating **1p** starts to aggregate. Besides confirming that C-terminal modification increases the self-assembling ability of **4**, these results reveal the characteristics of each C-terminal motif in the process of enzyme-instructed self-assembly, which is consistent with the trend of IC_{90} values (Fig. 4B).

Using sarcoma osteogenic (Saos-2) cells that overexpress alkaline phosphatase as a model for human cancer cells and human marrow stromal cells (HS-5) as a model for normal human cells, we test the anticancer efficacy and selectivity of **1p**, **2p**, **3p** and **4p**. While **4p** only inhibits Saos-2 cells at a high concentration (i.e., about 500 μM), **1p**, **2p** or **3p** inhibits Saos-2 at the concentration of 50 μM and above (Fig. 4A and Fig. S6). The IC_{90} values of **1p**, **2p**, **3p** and **4p** against Saos-2 cells are 36 μM , 97 μM , 37 μM , and 470 μM respectively (Fig. 4B), demonstrating that the C-terminal modification lower the IC_{90} against Saos-2 cells over an order of magnitude (from 470 μM of **4p** to 36 μM of **1p**). Since HS-5 hardly overexpress ALP, **1p**, **2p**, **3p** and **4p** all show limited cytotoxicity (i.e., $\text{IC}_{50} > 260\mu\text{M}$ (Fig. S7) and $\text{IC}_{90} > 500 \mu\text{M}$) on HS-5 cells. Moreover, the IC_{50} of **1p** (32 μM , 72 h) against Saos-2 is only about one-sixth of the IC_{50} of carboplatin (198 μM , 72 h),¹⁵ confirming that **1p** can exhibit a higher anticancer efficacy than that of a clinical used drug. Moreover, our study reveals that, at pH 8.0 and because of the hydrolysis of ester bond, the inhibitory activity of **3p** decreases, but the activity of **1p** remains (Fig. S8). These results agree with the self-assembling abilities of the D-tripeptides (Fig. 3B), thus validating C-terminal modification as an effective approach for developing enzyme-instructed self-assembly of short peptides for selectively inhibiting cancer cells.

To establish the essential role of enzymatic self-assembly of the D-tripeptide for their inhibitory activities, we co-incubate ALP inhibitors with the precursors during cell viability assay. We use two kinds of ALP inhibitors: levamisole for selectively inhibiting the activity of tissue-nonspecific alkaline phosphatase (ALPL),¹⁸ and L-phenylalanine (L-Phe) selectively for placental alkaline phosphatase (ALPP).¹⁹ As shown in Fig. 4C and Fig. S9, levamisole increases the cell viability of the Saos-2 cells treated by **1p** (50 μM), **3p** (50 μM), or **2p** (200 μM), while L-Phe is unable to rescue the cells. These results agree with previous

reports that levamisole largely inhibit the enzyme activity of phosphatase in Saos-2 cells,²⁰ confirming the importance of enzyme reaction in forming localized supramolecular assemblies of the D-tripeptide for cancer inhibition. In addition, with the help of Congo red—a dye for beta-sheet like, self-assembled nanofibers, we are able to visualize the nanofibers mainly formed in pericellular space of Saos-2 cells after treating the cells with the precursors **1p**, **2p** or **3p** (Fig. S11). This imaging results support localized enzyme-instructed self-assembly. Using a pan-caspase inhibitor (zVAD-fmk)²¹ and a necroptosis inhibitor (Nec-1)²², we further evaluate the modality of the death of Saos-2 cells resulted from the self-assemblies of the D-tripeptides (Fig. 4D and Fig. S10). Notably, Nec-1 significantly protects Saos-2 cells from the death caused by **1p**, **2p** and **3p**, suggesting that the cell death largely involve necroptosis. On the other hand, zVAD-fmk only slightly protects cells from **1p** (20 μ M), **2p** (50 μ M), and **3p** (20 μ M), indicating that the death of Saos-2 cells less relies on apoptosis when the precursor concentrations are relatively low.

In conclusion, this work illustrates C-terminal modification of short peptides as an effective approach to modulate the self-assembly of the peptides, thus providing a new dimension for exploring enzyme-instructed self-assembly for controlling the fate of cell. Moreover, the approach illustrated here should be useful for increasing the self-assembling ability of other self-assembling peptides and peptide conjugates.²³ In addition, this work illustrates that a simple control of molecular structures can have profound impact on multiple length scales, from nanometers to microns, which would help explore emergent properties of supramolecular assemblies in cellular environment, a new frontier of supramolecular chemistry. Because cell death caused by **2p/2** differs from that of **1p/1** or **p/3**, different C-terminal modifications likely result in subtle differences in supramolecular assemblies. This observation warrants further investigation since it may provide new insights on the use of supramolecular assemblies for inhibiting cancer cells.

Supplementary Material

Refer to Web version on PubMed Central for supplementary material.

Acknowledgments

This work was partially supported by NIH (CA142746) and W. M. Keck Foundation. ZF thanks the Dean's fellowship from Brandies University.

Notes and references

1. Vonhoff DD, Schilsky R, Reichert CM, Reddick RL, Rozenzweig M, Young RC, Muggia FM. *Cancer Treat Rep.* 1979; 63:1527–1531. [PubMed: 387223]
2. Kohn EC, Sarosy G, Bicher A, Link C, Christian M, Steinberg SM, Rothenberg M, Adamo DO, Davis P, Ognibene FP, Cunnion RE, Reed E. *J Natl Cancer Inst.* 1994; 86:18–24. [PubMed: 7505830]
3. Hodi FS, O'Day SJ, McDermott DF, Weber RW, Sosman JA, Haanen JB, Gonzalez R, Robert C, Schadendorf D, Hassel JC, Akerley W, van den Eertwegh AJM, Lutzky J, Lorigan P, Vaubel JM, Linette GP, Hogg D, Ottensmeier CH, Lebbe C, Peschel C, Quirt I, Clark JI, Wolchok JD, Weber JS, Tian J, Yellin MJ, Nichol GM, Hoos A, Urba WJ. *N Engl J Med.* 2010; 363:711–723. [PubMed: 20525992]

4. Kelderman S, Schumacher TNM, Haanen JBAG. *Mol Oncol*. 2014; 8:1132–1139. [PubMed: 25106088]
5. Wang H, Yang C, Wang L, Kong D, Zhang Y, Yang Z. *Chem Commun*. 2011; 47:4439–4441. Gao Y, Kuang Y, Guo ZF, Guo ZH, Krauss IJ, Xu B. *J Am Chem Soc*. 2009; 131:13576–13577. [PubMed: 19731909] Yang ZM, Xu KM, Guo ZF, Guo ZH, Xu B. *Adv Mater*. 2007; 17:3152–3156. Zhou J, Du X, Yamagata N, Xu B. *J Am Chem Soc*. 2016
6. Kuang Y, Shi J, Li J, Yuan D, Alberti KA, Xu Q, Xu B. *Angew Chem Int Ed*. 2014; 53:8104–8107.
7. Shi J, Du X, Yuan D, Zhou J, Zhou N, Huang Y, Xu B. *Biomacromolecules*. 2014; 15:3559–3568. [PubMed: 25230147]
8. Pires RA, Abul-Haija YM, Costa DS, Novoa-Carballal R, Reis RL, Ulijn RV, Pashkuleva I. *J Am Chem Soc*. 2015; 137:576–579. [PubMed: 25539667]
9. Tanaka A, Fukuoka Y, Morimoto Y, Honjo T, Koda D, Goto M, Maruyama T. *J Am Chem Soc*. 2015; 137:770–775. [PubMed: 25521540]
10. Kuang Y, Xu B. *Angew Chem Int Ed Engl*. 2013; 52:6944. [PubMed: 23686848]
11. Kuang Y, Long MJ, Zhou J, Shi J, Gao Y, Xu C, Hedstrom L, Xu B. *J Biol Chem*. 2014; 289:29208–29218. [PubMed: 25157102]
12. Du X, Zhou J, Shi J, Xu B. *Chem Rev*. 2015; 115:13165–13307. [PubMed: 26646318]
13. Gao J, Wang H, Wang L, Wang J, Kong D, Yang Z. *J Am Chem Soc*. 2009; 131:11286–11287. [PubMed: 19630424] Zhao F, Gao Y, Shi J, Browdy HM, Xu B. *Langmuir*. 2011; 27:1510–1512. [PubMed: 21138331]
14. Tardito S, Isella C, Medico E, Marchio L, Bevilacqua E, Hatzoglou M, Bussolati O, Franchi-Gazzola R. *J Biol Chem*. 2009; 284:24306–24319. [PubMed: 19561079]
15. Marley K, Helfand SC, Edris WA, Mata JE, Gitelman AI, Medlock J, Seguin B. *BMC Vet Res*. 2013; 9. [PubMed: 23311963]
16. Linkermann A, Green DR. *N Engl J Med*. 2014; 370:455–465. [PubMed: 24476434] Vanden Berghe T, Linkermann A, Jouan-Lanhouet S, Walczak H, Vandenabeele P. *Nat Rev Mol Cell Biol*. 2014; 15:134–146.
17. Du X, Zhou J, Wu L, Sun S, Xu B. *Bioconjugate Chem*. 2014; 25:2129–2133.
18. Kozlenkov A, Le Du MH, Cuniasso P, Ny T, Hoylaerts MF, Millan JL. *J Bone Miner Res*. 2004; 19:1862–1872. [PubMed: 15476587]
19. Hoylaerts MF, Manes T, Millan JL. *Biochem J*. 1992; 286:23–30. [PubMed: 1520273]
20. Murray E, Provvedini D, Curran D, Catherwood B, Sussman H, Manolagas S. *J Bone Miner Res*. 1987; 2:231–238. [PubMed: 2843003]
21. Slee EA, Zhu HJ, Chow SC, MacFarlane M, Nicholson DW, Cohen GM. *Biochem J*. 1996; 315:21–24. [PubMed: 8670109]
22. Kammuller ME, Seinen W. *Int J Immunopharmacol*. 1988; 10:997–1010. [PubMed: 3215711] Degtrev A, Huang ZH, Boyce M, Li YQ, Jagtap P, Mizushima N, Cuny GD, Mitchison TJ, Moskowitz MA, Yuan JY. *Nat Chem Biol*. 2005; 1:112–119. [PubMed: 16408008]
23. Jiang T, Vail OA, Jiang Z, Zuo X, Conticello VP. *J Am Chem Soc*. 2015; 137:7793–7802. [PubMed: 26021882] Liang C, Ni R, Smith JE, Childers WS, Mehta AK, Lynn DG. *J Am Chem Soc*. 2014; 136:15146–15149. [PubMed: 25313920] Sathaye S, Zhang H, Sonmez C, Schneider JP, MacDermid CM, Von Bargen CD, Saven JG, Pochan DJ. *Biomacromolecules*. 2014; 15:3891–3900. [PubMed: 25251904] Smith DJ, Brat GA, Medina SH, Tong D, Huang Y, Grahmmer J, Furtmueller GJ, Oh BC, Nagy-Smith KJ, Walczak P, Brandacher G, Schneider JP. *Nat Nanotechnol*. 2016; 11:95–102. [PubMed: 26524396] Sun Z, Li Z, He Y, Shen R, Deng L, Yang M, Liang Y, Zhang Y. *J Am Chem Soc*. 2013; 135:13379–13386. [PubMed: 23984683] Cui H, Cheatham AG, Pashuck ET, Stupp SI. *J Am Chem Soc*. 2014; 136:12461–12468. [PubMed: 25144245] Foster JS, Zurek JM, Almeida NMS, Hendriksen WE, le Sage VAA, Lakshminarayanan V, Thompson AL, Banerjee R, Eelkema R, Mulvana H, Paterson MJ, van Esch JH, Lloyd GO. *J Am Chem Soc*. 2015; 137:14236–14239. [PubMed: 26502267] Zhang X, Chu X, Wang L, Wang H, Liang G, Zhang J, Long J, Yang Z. *Angew Chem, Int Ed*. 2012; 51:4388–4392. He M, Li J, Tan S, Wang R, Zhang Y. *J Am Chem Soc*. 2013; 135:18718–18721. [PubMed: 24106809] Yu Z, Tantakitti F, Yu T, Palmer LC, Schatz GC, Stupp SI. *Science*. 2016; 351:497–502. [PubMed: 26823427]

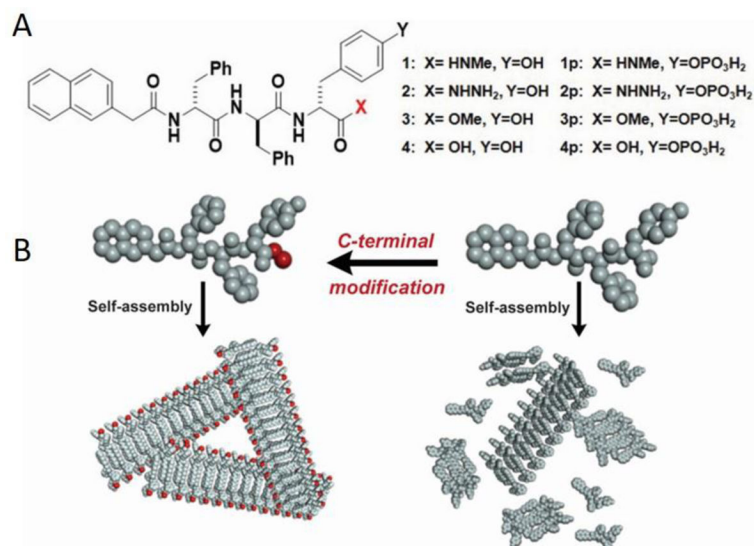


Fig. 1.
 A) Molecular structures of self-assembling short peptides **1**, **2**, **3** and **4** and the corresponding precursors **1p**, **2p**, **3p** and **4p** that are enzyme substrates; B) Illustration of C-terminal modification enhancing self-assembly.

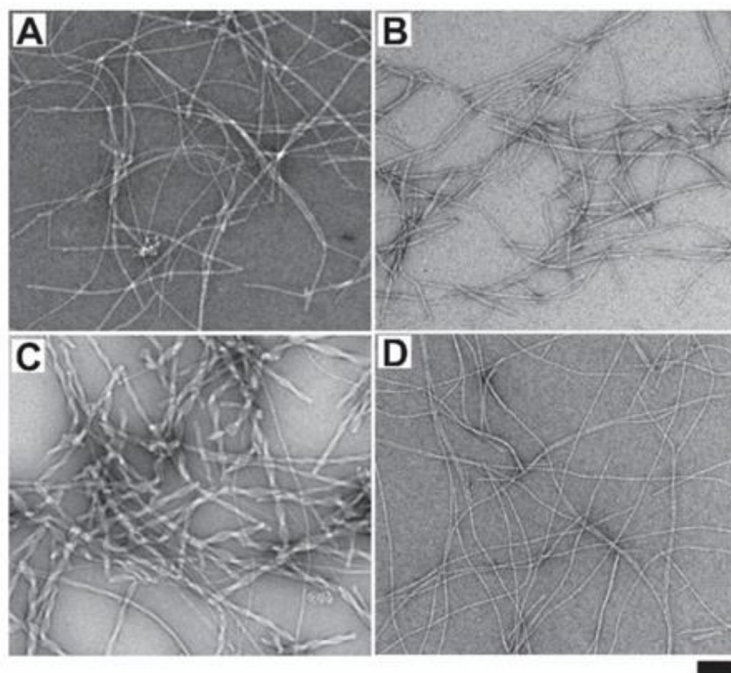


Fig. 2. TEM images of the nanostructures formed by adding ALP (3 U/mL) into the aqueous solution (1 mM, pH 7.4) of (A) **1p**, (B) **2p**, (C) **3p**, and (D) **4p** after 24 hrs, respectively (scar bar 100 nm).

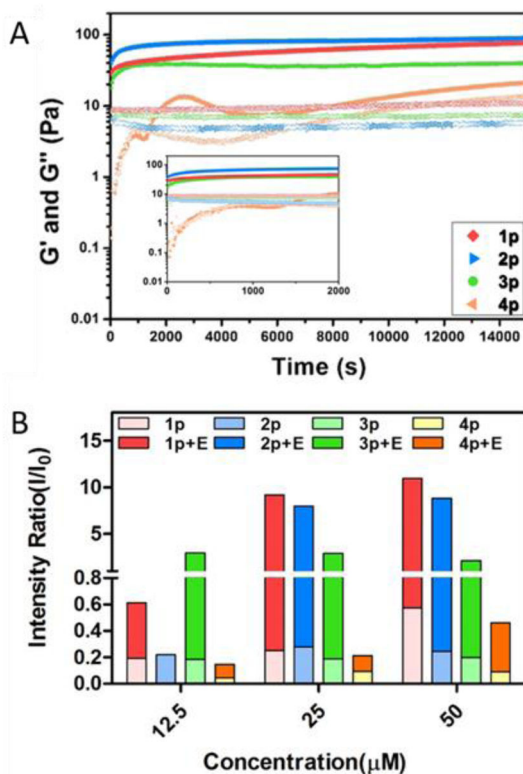


Fig. 3.

A) Storage modulus (G' -solid symbol) and loss modulus (G'' -open symbol) as a function of time for 0.5 wt % of **1p**, **2p**, **3p** and **4p** catalyzed by ALP (0.05 U/mL) at pH7.4. Inset: enlarged time sweep between 0 to 2000 seconds; B) Intensity of static light scattering (SLS) of the solutions of **1p**, **2p**, **3p** and **4p** (12.5–50 μM) before and after adding ALP (2 U/mL) for 24 hours at different concentrations in pH7.4 PBS buffer (light scattering angle = 30 degree).

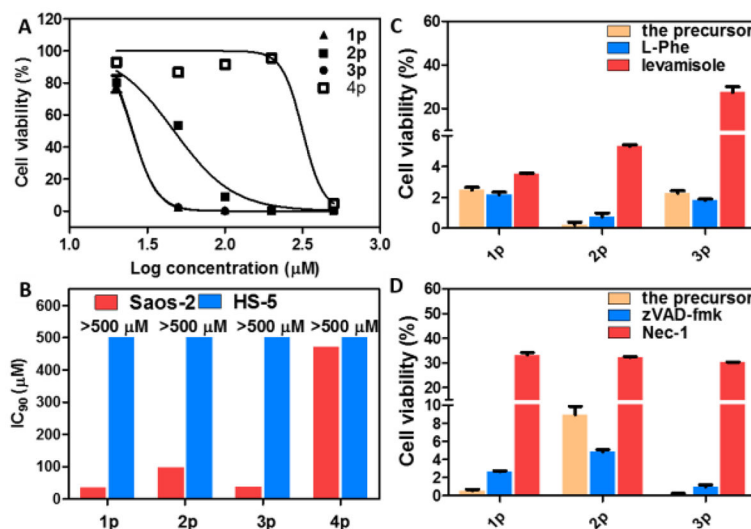


Fig. 4.

A) Cell viability (log-dose response curves) for sarcoma osteogenic (Saos-2) cells treated with **1p**, **2p**, **3p** or **4p**. B) IC₉₀ values (48 h) of **1p**, **2p**, **3p**, and **4p** against Saos-2 and HS-5 cells. C) The cell viability of Saos-2 cells treated with **1p** (50 μM), **2p** (200 μM), or **3p** (50 μM) in the presences of different ALP inhibitors (L-Phe and levamisole). Cells were treated for 48h; [L-Phe] = 1 mM; [levamisole] = 1 mM. D) The cell viability of Saos-2 cells treated with **1p**, **2p**, or **3p** (100 μM) in the presence of a pan-caspase inhibitor (zVAD-fmk) or a necroptosis inhibitor (Nec-1). Cells were treated for 48h; [zVAD-fmk] = 45 μM; [Nec-1] = 50 μM. All cell viability test are done in triplicate (n = 3).